

Microstructures and Failure Mechanisms of Spot Friction Welds in Lap-Shear Specimens of Aluminum 5754 Sheets

S. G. Arul, T. Pan

Ford Motor Company

P.-C. Lin, J. Pan

University of Michigan

Z. Feng, M. L. Santella

Oak Ridge National Laboratory

Copyright © 2005 Society of Automotive Engineers, Inc.

ABSTRACT

Microstructures and failure mechanisms of spot friction welds (SFW) in aluminum 5754 lap-shear specimens were investigated. In order to study the effect of tool geometry on the joint strength of spot friction welds, a concave tool and a flat tool were used. In order to understand the effect of tool penetration depth on the joint strength, spot friction welds were prepared with two different penetration depths for each tool. The results indicated that the concave tool produced slightly higher joint strength than the flat tool. The joint strength did not change for the two depths for the flat tool whereas the joint strength slightly increases as the penetration depth increases for the concave tool. The experimental results show that the failure mechanism is necking and shearing for the spot friction welds made by both tools. The failure was initiated and fractured through the upper sheet under the shoulder indentation near the crack tip.

INTRODUCTION

Automotive companies are continuously substituting conventional steel with advanced high strength steel (AHSS), aluminum, magnesium, and composites to reduce the vehicle weight. In the body structure, aluminum and composites are replacing steel for closure panels such as hood, deck lid, etc., and AHSS is replacing conventional steel for structural components such as B-pillar, underbody cross members, etc.

For a typical body construction, resistance spot welding (RSW) is the joining process to combine various sheet metal parts. However, resistance spot welding is not the best process for joining sheet metal parts made of aluminum. Resistance spot welding on aluminum sheets likely produces poor welds, as reported in Thornton et al. [1] and Gean et al. [3]. Therefore, the automotive

industry has been using structural adhesives, rivets, toggle-lock, etc. to join aluminum panels. These processes require longer cycle time and are costlier than the conventional resistance spot welding process.

Recently, Mazda introduced a new process, spot friction welding (SFW), for joining aluminum panels. A schematic diagram of the spot friction welding process is shown in Figure 1 [4,5]. As shown in Figure 1, a rotating tool with a probe is plunged into the upper sheet. The lower sheet is supported by a backing tool to support the downward force from the probing tool. The downward force and the rotational speed are maintained for an appropriate time to generate frictional heat. Then heated and softened material adjacent to the tool deforms plastically, and a solid state bond is made between the surfaces of the upper and lower sheets. Note that the spot friction welding process is less capital intensive compared to the resistance spot welding process and it has a shorter cycle time than the rivet and toggle lock processes.

In automotive body panels, two common types of aluminum sheets are used: 6xxx series, heat treatable alloys, used for parts such as hoods, deck lids and other outer panels, and 5xxx series, non-heat treatable alloys, used for parts such as latch and hinge reinforcements. There have been a lot of efforts to understand the joint strength, microstructures and failure mechanisms of spot friction welds. For example, Lin et al. [2] showed in details the factors affecting the joint strength of spot friction welds in lap-shear specimens of aluminum 6111-T4 sheets. They also presented the microstructures and failure mechanisms of spot friction welds under various process conditions.

In this paper, microstructures and failure mechanisms of spot friction welds in aluminum 5754 lap-shear

specimens are investigated based on experimental observations. Two types of tools, a flat tool and a concave tool, were used. Micrographs of spot friction welds made by the two types of tools in lap-shear specimens before and after failure are obtained. Joint strengths for spot friction welds made by the two types of tools with different penetration depths are then presented and compared. Finally, the failure modes and failure mechanisms for these spot friction welds are discussed.

EXPERIMENT

In this investigation, aluminum 5754 sheets with a thickness of 1.0 mm were used. Lap-shear specimens were made by using two 25.4 mm by 101.6 mm sheets with a 25.4 mm by 25.4 mm overlap area. Spot friction welds were made by a friction stir welding system manufactured by MTS[®] Systems Corporation, as shown in Figure 2. This equipment is capable of controlling either force or displacement to achieve proper welds. This machine can be used to make linear, non-linear, and spot welds.

For spot friction welding (SFW), the important processing variables are tool geometry, rotational speed, tool holding time and downward (normal) force. The tool holding time and the normal force can be related by the penetration depth of the tool. As illustrated in Figure 3, the rotational speed (rpm) for the duration of the weld process is held constant while the maximum displacement of the tool, the penetration depth, can be varied to produce different welds. As schematically shown in Figure 3, at time, t_0 , the tool contacts the top surface of the specimen. Then, the displacement increases linearly until it reaches the maximum displacement at t_1 . The normal force generally increases with the increase of displacement as schematically shown in Figure 3.

The spot friction welding system has two components: a rotational tool located above the upper sheet and a stationary anvil located beneath the lower sheet, as shown in Figure 4. The rotational tool has two features: a probing pin which is used to penetrate into the specimen and a shoulder which is used to generate frictional heat and spreads the metal in the stir zone. The shape of the shoulder controls the material flow around the pin and shoulder.

In this investigation, a tool with a concave shoulder and a tool with a flat shoulder were used. In order to study the effect of the penetration depth, the specimens were made with two different depths of 1.85 mm and 1.95 mm. Four sets of welds were produced under the four process conditions as listed in Table 1.

The lap-shear specimens were tested to obtain the shear strength by using an Instron[®] Model 4502 testing machine. The crosshead displacement was set at a rate of 10.0 mm per minute. The load and displacement were simultaneously recorded during the test. Tests

were terminated when the maximum loads were reached. A typical load-displacement curve for a specimen made by the concave tool with the penetration depth of 1.85 mm is shown in Figure 5. This load-displacement curve can be divided into three distinct regions: in Region 1, the slackness in the test set up is removed. Then, in Region 2, the load increases rapidly. Finally, in Region 3, significant plastic deformation takes place under the probing tool and the maximum load is reached.

The average maximum loads (joint strengths) for all the four conditions are listed in Table 2. With the concave tool, the maximum load increases by approximately 4.7% (3.06 kN vs. 2.92 kN) when the depth increases from 1.85 mm to 1.95 mm. However, with the flat tool, the maximum loads stay the same (2.88 kN) for the depths of 1.95 mm and 1.85 mm. For the depth of 1.85 mm, the maximum load for the concave tool is larger than that for the flat tool by 1% (2.92 kN vs. 2.88 kN). For the depth of 1.95 mm, the maximum load for the concave tool is larger than that of the flat tool by 6.3% (3.06 kN vs. 2.88 kN).

MICROSTRUCTURES AND FAILURE MECHANISMS

Figure 6(a) shows the micrograph of the cross section of a spot friction weld made by the concave tool before testing. Near the center, the shape of the indentation matches the profile of the probe pin and the shoulder. With the concave shoulder, the shoulder squeezes a lot of material from upper sheet metal to the location near the probe. The light gray area around the pin and the shoulder represents the stir zone and the slightly darker area surrounding the stir zone is the thermal-mechanical affected zone. Two notch tips at the unwelded interface between the upper and lower sheets near the spot friction weld are denoted by C and D.

Figure 6(b) shows the micrograph of the cross section of a spot friction weld made by the flat tool before testing. Near the center, the shape of the indentation matches the profile of the tool pin and the shoulder. With the flat shoulder, the upper sheet metal near the shoulder is almost flat except near the tool hole. The light gray area around the pin and the shoulder represents the stir zone and the slightly darker area surrounding the stir zone is the thermal-mechanical affected zone. Two notch tips at the unwelded interface between the upper and lower sheets near the spot friction weld are denoted by E and F.

A comparison of Figures 6(a) and 6(b) shows that the stir zone for the concave tool (light gray area around the probe and the shoulder) is much larger compared to that of the flat tool, as observed for spot friction welds in aluminum 6111-T4 sheets by Lin et al [2]. As shown in Figures 6(a) and 6(b), due to different flow patterns, the shapes of the interface between the upper and lower sheets under the shoulder indentation are quite different. The different flow patterns also result in different shapes of spot friction welds as shown in Figures 6(a) and 6(b).

For both cases, we also observed that the flow of the upper sheet material due to the shoulder indentation during the process results in a bend of the upper sheet just outside the shoulder indentation.

The geometries of the stir zone and thermal-mechanical affected zone change according to the tool geometry and penetration depth. However, the microstructures in the stir zones appear to be similar in the welds under the four process conditions. The microstructures in the thermal-mechanical affected zones also appear to be similar in the welds under the four process conditions. Figure 7 shows the micrographs of a spot friction weld made by the concave tool with the depth of 1.95 mm as a representative case. Figure 7(a) shows again the micrograph of the entire cross section. The boxed areas indicate where the grain structure samples are taken to show the details of the stir zone and thermal-mechanical affected zone. A close-up view of the stir zone in Figure 7(b) shows very fine equiaxed grains. This is due to stirring and recrystallization. A close-up view of the thermal-mechanical affected zone in Figure 7(c) shows fine grains. For comparison, a close-up view of the base metal in Figure 7(d) shows coarse grains.

Figure 8 shows a cross sectional view and close-up views of a spot friction weld made by the concave tool with the depth of 1.95 mm in a partially failed lap-shear specimen. The two arrows in Figure 8(a) schematically show the loading direction. In Figure 8(a), near the upper right portion of the spot friction weld, marked as Leg 2, a necking and shearing failure appears at point A. The necking and shearing failure mechanism is very similar to that of the failed resistance spot welds in lap-shear specimens in Lin et al. [7]. Note that the location of the necking and shearing failure is close to the outer circumference of the shoulder indentation near the crack tip. In Figure 8(b), a close-up view of region I shows the necking failure. In Figure 8(c), a magnified view of region II shows the microstructures near the crack tip. Note that the material in the lower portion of region II appears to be the base metal and the material in the upper left portion of region II appears to be the thermal-mechanical affected zone.

Figure 9 shows a cross sectional view and close-up views of a spot friction weld made by the flat tool with the depth of 1.95 mm in a partially failed lap-shear specimen. The two arrows in Figure 9(a) schematically show the loading direction. In Figure 9(a), near the upper left portion of the spot friction weld, marked as Leg 1, a necking and shearing failure appears at point A. The necking and shearing failure mechanism is very similar to that of the failed resistance spot welds in lap-shear specimens in Lin et al. [7]. Note that the location of the necking and shearing failure is closer to the center of the spot friction weld under the shoulder indentation when compared to that shown in Figure 8(a). In Figure 9(b), a close-up view of region I shows the necking and shear failure. In Figure 9(c), a magnified view of region II shows the microstructures near the crack tip. Note that the failure profiles shown in Figures 9(b) and 9(c) do

not seem to match. It is possible that when sample was prepared for micrographs, the upper left sheet was distorted. The cross section of the upper left sheet and the cross section of the weld nugget as shown may come from different locations along the weld circumference. Therefore, the failure profiles do not match.

For both the specimens made by the concave and flat tools, the necking and shearing failure mechanism is the principal failure initiation mechanism, similar to the study for the spot friction welds in aluminum 6111-T4 sheets [6]. Note that due to the limited ductility, a combined mode of necking and shearing localization is the principal failure mechanism of aluminum 5754 and 6111-T4 sheets under biaxial stretching conditions as indicated in Chien et al. [8].

CONCLUSIONS

Microstructures and failure mechanisms of spot friction welds in aluminum 5754 lap-shear specimens were investigated based on experimental observations. In order to understand the effect of tool geometry on the joint strength, a concave tool and a flat tool were used. In order to understand the effect of the penetration depth on the joint strength, two depths of 1.85 mm and 1.95 mm were selected. The experimental results showed that the joint strength is slightly higher for the concave tool for the two depths. For the flat tool, the joint strengths remain the same for the two depths. For the concave tool, the joint strength increases when the depth increases from 1.85 mm to 1.95 mm. All specimens exhibit the necking and shearing failure mechanism. The failure was initiated and fractured through the upper sheet under the shoulder indentation near the crack tip.

ACKNOWLEDGEMENT

The assistance of A. Joaquin, R. Cooper and D. Houston of Ford Motor Company for their help in the experiment is greatly appreciated. The support of C. Johnson, J. Helms and C. Wu of Ford Motor Company for this project is also appreciated. The support of this work at University of Michigan by a grant from the Ford University Research Program is greatly appreciated. This research was also sponsored in part by the U.S. Department of Energy, Assistant Secretary for Energy Efficiency and Renewable Energy, Office of FreedomCAR and Vehicle Technologies, as part of High Strength Weight Reduction Materials Program under Contract DE-AC05-00OR22725 with UT-Battelle, LLC. The DOE Technology Development Area Specialist is S. Diamond, and the Field Technical Manager is P. S. Sklad.

REFERENCES

- 1 Thornton, P., Krause, A. and Davies, R., 1996, "Aluminum Spot Weld". Welding Journal, Vol. 75, pp. 101s-108s.
- 2 Lin, P.-C., Lin, S.-H., Pan, J., Pan, T., Nicholson, J. M., Garman, M. A., "Microstructures and Failure Mechanisms of Spot Friction Welds in Lap-Shear Specimens of Aluminum 6111-T4 Sheets". SAE Technical Paper No: 2004-01-1330, Society of Automotive Engineers, Warrendale, PA.
- 3 Gean, A., Westgate, S. A., Kucza, J. C. and Ehrstorm, J. C., 1999, "Static and Fatigue Behavior of Spot-Welded 5182-0 Aluminum Alloy Sheet". Welding Journal, Vol. 78, pp. 80s-86s.
- 4 Sakano, R., Murakami, K., Yamashita, K., Hyoe, T., Fujimoto, M., Inuzuka, M., Nagao, Y. and Kashiki, H., 2001, "Development of Spot FSW Robot System for Automobile Body Members". Proceedings of the 3rd International Symposium of Friction Stir Welding, Kobe, Japan, September 27-28, 2001.
- 5 Iwashita, T., 2003, "Method and apparatus for joining". US Patent 6601751 B2, August, 5, 2003.
- 6 Lin, P.-C., Lin, S.-H. and Pan, J., 2004, "Modeling of Plastic Deformation and Failure near Spot Welds in Lap-Shear Specimens". SAE Technical Paper no. 2004-01-0817, Society of Automotive Engineers, Warrendale, PA.
- 7 Lin, S.-H., Pan, J., Tyan, T. and Prasad, P., 2003, "A General Failure Criterion for Spot Welds under Combined Loading Conditions". International Journal of Solids and Structures, Vol. 40, pp. 5539-5564.
- 8 Chien, W. Y., Pan, J. and Tang, S. C., 2004, "A Combined Necking and Shear Localization Analysis for Aluminum Sheets under Biaxial Stretching Conditions". International Journal of Plasticity, Vol. 20, pp. 1953-1981.

CONTACT

Senthil G. Arul, TVM, Ford Motor Company, Dearborn, MI 48101. Telephone/Fax: (313) 845-9219, Email: sarul@ford.com.

Condition	Tool	Depth
1	Concave	1.85 mm
2	Concave	1.95 mm
3	Flat	1.85 mm
4	Flat	1.95 mm

Table 1. Four processing conditions.

Depth	Concave tool	Flat tool
1.85 mm	2.92 kN	2.88 kN
1.95 mm	3.06 kN	2.88 kN

Table 2. A comparison of joint strengths for spot friction welds made by two types of tools with two different depths under lap-shear loading conditions.

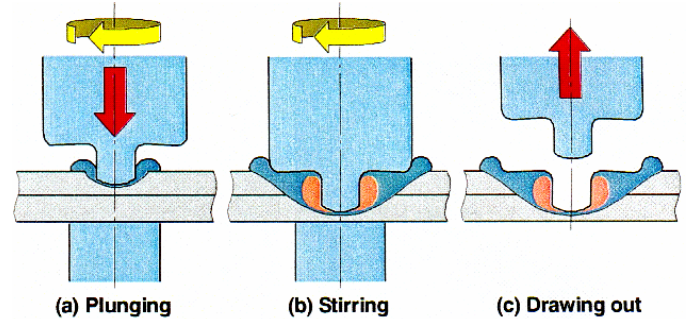


Figure 1. A schematic illustration of spot friction welding (SFW) process.



Figure 2. A friction stir welding system manufactured by MTS® Systems Corporation.

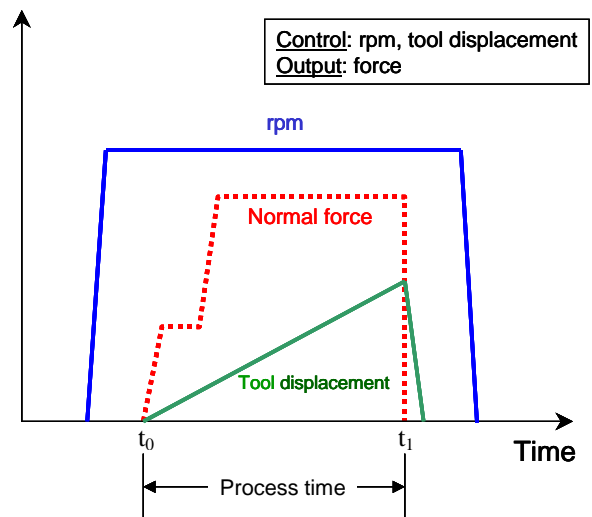
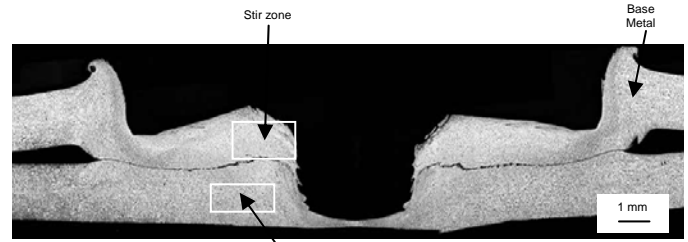
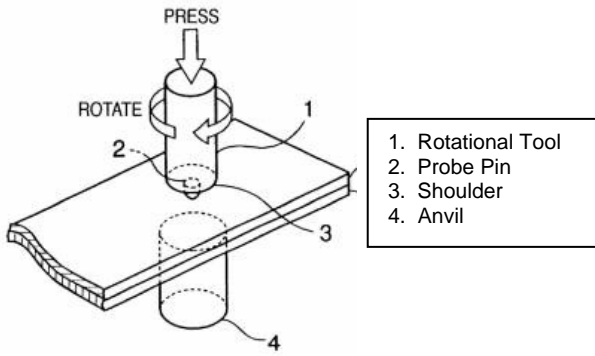


Figure 3. A schematic plot of the process parameters (rpm, normal force, and tool displacement) as a function of time.



(a)

Figure 4. A schematic plot of a spot friction welding system.

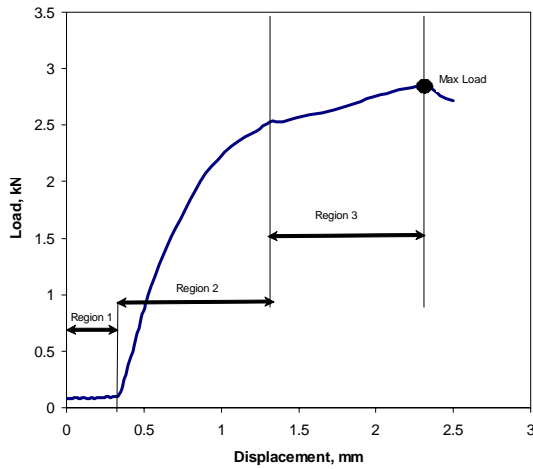
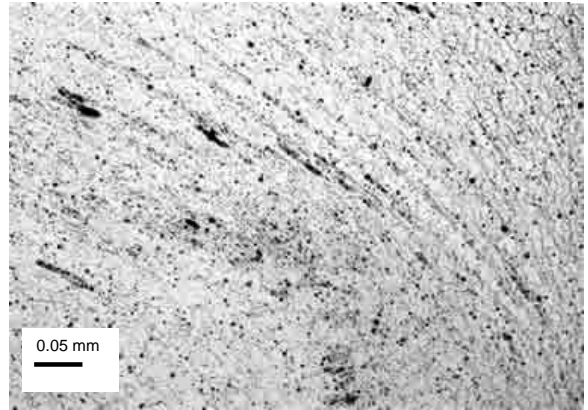
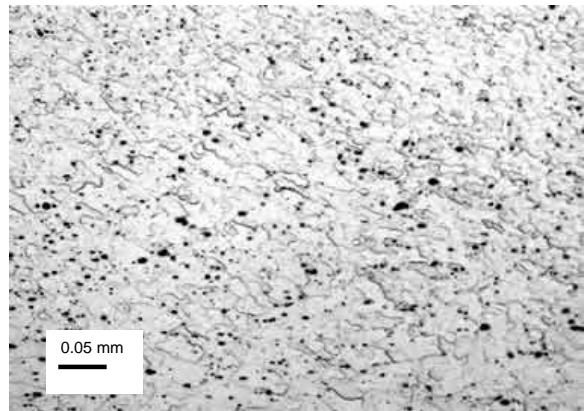


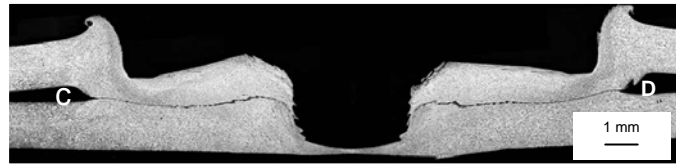
Figure 5. A load-displacement curve of a spot friction weld made by the concave tool with the depth of 1.85 mm.



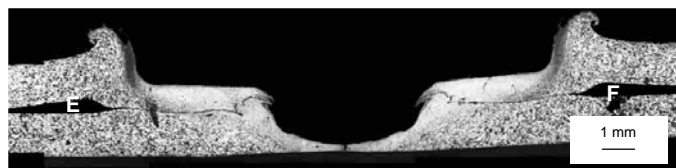
(b)



(c)

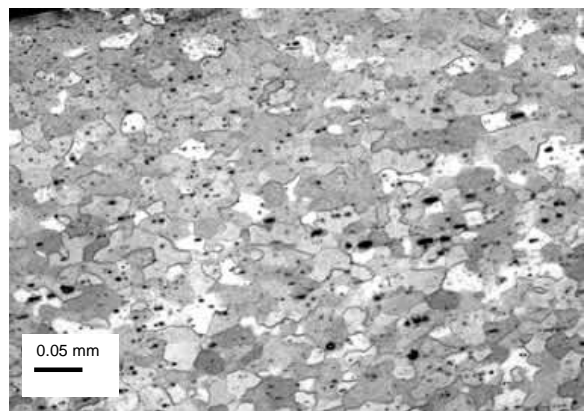


(a)



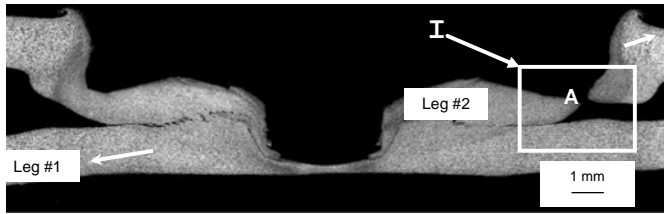
(b)

Figure 6. (a) A micrograph of the cross section of a spot friction weld made by the concave tool with the depth of 1.95 mm, (b) a micrograph of the cross section of a spot friction weld made by the flat tool with the depth of 1.95 mm.

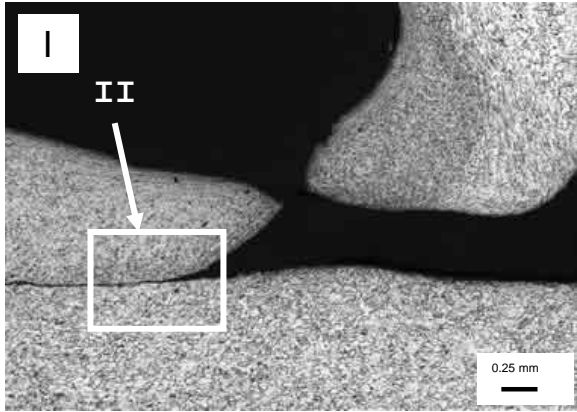


(d)

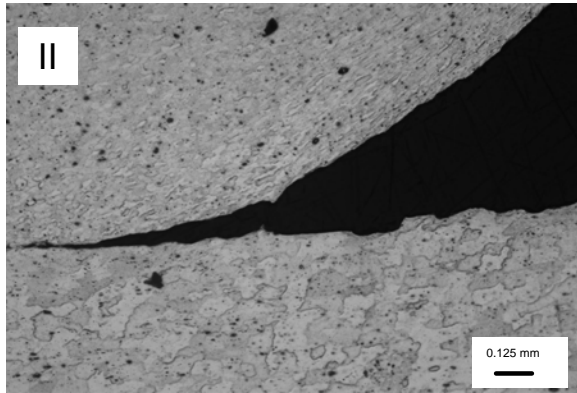
Figure 7. (a) A micrograph of the cross section of a spot friction weld made by the concave tool with the depth of 1.95 mm, (b) A close-up view of the stir zone, (c) a close-up view of the thermal-mechanical affected zone, (d) a close-up view of the base metal.



(a)

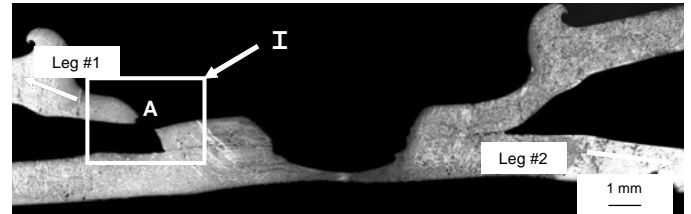


(b)

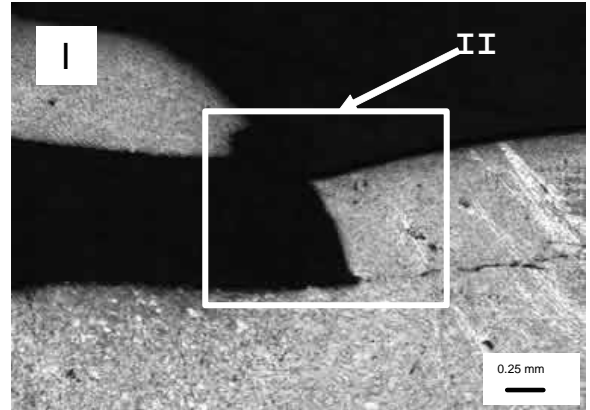


(c)

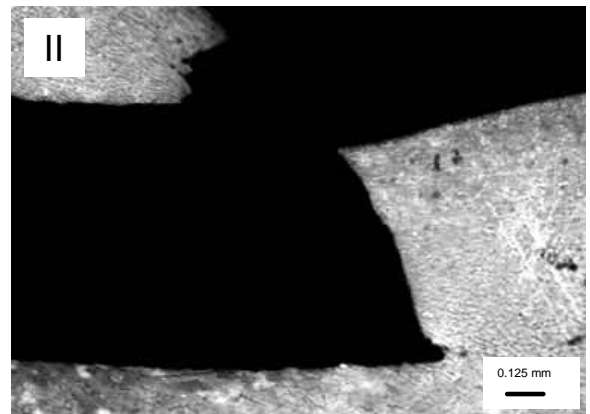
Figure 8. A micrograph of the cross section of a spot friction weld made by the concave tool with the depth of 1.95 mm in a partially failed lap-shear specimen, (b) a close-up view of region I, (c) a close-up view of region II.



(a)



(b)



(c)

Figure 9. A micrograph of the cross section of a spot friction weld made by the flat tool with the depth of 1.95 mm in a partially failed lap-shear specimen, (b) a close-up view of region I, (c) a close-up view of region II.